

US Patent & Trademark Office
Patent Public Search | Text View

United States Patent	12392855
Kind Code	B2
Date of Patent	August 19, 2025
Inventor(s)	Zheng; Hang et al.

Two-dimensional direction-of-arrival estimation method for coprime surface array based on virtual domain tensor filling

Abstract

Disclosed in the present invention is a two-dimensional direction-of-arrival estimation method for a coprime surface array based on virtual domain tensor filling, which mainly solves the problems of the loss of multi-dimensional signal structural information and the inability to fully utilize virtual domain statistics in the existing method. The steps thereof are as follows: constructing a coprime surface array; modeling a tensor of a received signal of the coprime surface array; constructing an augmented non-continuous virtual surface array based on cross-correlation tensor transformation of the coprime surface array; deriving a virtual domain tensor based on mirror extension of the non-continuous virtual surface array; dispersing contiguous missing elements by reconstructing the virtual domain tensor; filling the virtual domain tensor based on the minimization of a tensor kernel norm; and decomposing a filled virtual domain tensor to obtain a direction-of-arrival estimation result.

Inventors:	Zheng; Hang (Zhejiang, CN), Zhou; Chengwei (Zhejiang, CN), Shi; Zhiguo (Zhejiang, CN), Wang; Yong (Zhejiang, CN), Chen; Jiming (Zhejiang, CN)
Applicant:	Zhejiang University (Zhejiang, CN)
Family ID:	1000008762580
Assignee:	Zhejiang University (Zhejiang, CN)
Appl. No.:	17/920401
Filed (or PCT Filed):	February 16, 2022
PCT No.:	PCT/CN2022/076430
PCT Pub. No.:	WO2023/137812
PCT Pub. Date:	July 27, 2023

Prior Publication Data

Document Identifier	Publication Date
US 20240210510 A1	Jun. 27, 2024

Foreign Application Priority Data

CN	202210077881.1	Jan. 21, 2022
----	----------------	---------------

Publication Classification

Int. Cl.:	G01S3/14 (20060101)
U.S. Cl.:	
CPC	G01S3/143 (20130101);

Field of Classification Search

USPC:	None
-------	------

References Cited

U.S. PATENT DOCUMENTS

Patent No.	Issued Date	Patentee Name	U.S. Cl.	CPC
2003/0058153	12/2002	Yu	N/A	N/A
2016/0172767	12/2015	Ray	N/A	N/A

FOREIGN PATENT DOCUMENTS

Patent No.	Application Date	Country	CPC
------------	------------------	---------	-----

104749552	12/2014	CN	N/A
106896340	12/2016	CN	N/A
107037392	12/2016	CN	N/A
107102291	12/2016	CN	N/A
107315160	12/2016	CN	N/A
107329108	12/2016	CN	N/A
107422295	12/2016	CN	N/A
107589399	12/2017	CN	N/A
108344967	12/2017	CN	N/A
108710102	12/2017	CN	N/A
109143152	12/2018	CN	N/A
109143228	12/2018	CN	N/A
110244259	12/2018	CN	N/A
110927661	12/2019	CN	N/A
111610486	12/2019	CN	N/A
111624545	12/2019	CN	N/A
112904272	12/2020	CN	N/A

OTHER PUBLICATIONS

“International Search Report (Form PCT/ISA/210) of PCT/CN2022/076430,” mailed on Jul. 27, 2022, pp. 1-5. cited by applicant

“Written Opinion of the International Searching Authority (Form PCT/ISA/237) of PCT/CN2022/076430,” mailed on Jul. 27, 2022, pp. 1-4. cited by applicant

Primary Examiner: Moore; Whitney

Attorney, Agent or Firm: JCIPRNET

Background/Summary

CROSS-REFERENCE TO RELATED APPLICATION

(1) This application is a 371 of international application of PCT application serial no. PCT/CN2022/076430, filed on Feb. 16, 2022, which claims the priority benefit of China application no. 202210077881.1, filed on Jan. 21, 2022. The entirety of each of the above mentioned patent applications is hereby incorporated by reference herein and made a part of this specification.

BACKGROUND

Technical Field

(2) The present invention belongs to the technical field of array signal processing and relates to a statistical signal processing technology based on sparse array virtual domain second-order high-dimensional statistics, in particular to a two-dimensional direction-of-arrival estimation method for coprime surface array based on virtual domain tensor filling, which can be used for target positioning.

Description of Related Art

(3) As a sparse array with a systematic structure, a coprime array has the advantages of a large aperture, and high resolution. It can break through the performance bottleneck of traditional uniform array direction-of-arrival estimation in estimation performance and cost overhead. Since sparsely arranged array elements of the coprime array do not meet a Nyquist sampling rate, in order to realize a Nyquist matching direction-of-arrival estimation, a common practice is to calculate second-order statistics of a received signal of the coprime array to construct an augmented non-contiguous virtual array, and extract a continuous part therefrom to realize Nyquist matching processing based on a virtual domain second-order equivalent signal. Further, in order to make full use of all the non-contiguous virtual array elements, an existing method fills a non-contiguous virtual array to improve the performance of the direction-of-arrival estimation. However, the above method usually expresses the received signal as a vector, and derives the virtual domain second-order equivalent signal by vectorizing a covariance matrix of the received signal; in a scenario where a coprime surface array is deployed, since the received signal of the coprime surface array covers two-dimensional spatial information, this vectorized signal processing method destroys an original spatial information structure of the received signal of the coprime surface array, which will cause serious performance loss.

(4) In order to preserve the structured information of the multi-dimensional received signal, a tensor, as a multi-dimensional data type, has been used in the field of array signal processing to characterize a received signal covering the multi-dimensional spatial information, and to perform feature analysis and effective information extraction, so as to achieve a high-precision and high-resolution direction-of-arrival estimation. However, when it relates to the statistic processing of the virtual field tensor of the coprime surface array, the augmented multi-dimensional non-contiguous virtual array would have holes in the whole piece, resulting in the corresponding virtual field tensor with contiguous missing elements. The traditional tensor filling method applied to image inpainting is premised on a random distribution of the missing elements in the tensor, so it cannot effectively fill the virtual field tensor. Therefore, for a virtual domain tensor model of the coprime surface array, how to effectively use all the non-continuous virtual domain tensor statistics information to achieve high-precision and high-resolution two-dimensional direction-of-arrival estimation is still an urgent problem to be solved.


SUMMARY

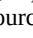
(5) The purpose of the present invention is to propose a two-dimensional direction-of-arrival estimation method for a coprime surface array based on virtual domain tensor filling in order to solve the problems of loss of multi-dimensional signal structure information and inability to fully utilize virtual domain statistics in existing methods. It provides a feasible idea and an effective solution to realize the high-precision and high-resolution two-dimensional direction-of-arrival estimation of Nyquist matching by making full use of all the non-continuous virtual domain tensor statistics information corresponding to the coprime surface array.

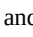
(6) The purpose of the present invention is to realize through the following technical solutions: a two-dimensional direction-of-arrival estimation method for a coprime surface array based on virtual domain tensor filling, wherein the method comprises the following steps: (1) using $4M_{\text{sub},x} \times N_{\text{sub},x} + N_{\text{sub},y} - 1$ physical antenna array elements by a receiving end, and performing constructing according to a structure of a coprime surface array, wherein $M_{\text{sub},x}$, $N_{\text{sub},x}$ and $M_{\text{sub},y}$, $N_{\text{sub},y}$ are a pair of coprime integers respectively; decomposing the coprime surface array into two sparse uniform sub-surface arrays $2M_{\text{sub},x} \times 2M_{\text{sub},y}$ antenna array elements, array element spacings in an x axial direction and a y axial direction are respectively $N_{\text{sub},x}d$ and $N_{\text{sub},y}d$, $N_{\text{sub},x} \times N_{\text{sub},y}$ antenna array elements, array element spacings in the x axial direction and the y axial direction are respectively $M_{\text{sub},x}d$ and $M_{\text{sub},y}d$, and the unit interval d is taken as half of the wavelength λ of an incident narrowband signal, that

is, $d=\lambda/2$; (2) assuming that there are K far-field narrowband signal sources from $\{(\theta.\text{sub}.1, \phi.\text{sub}.1), (\theta.\text{sub}.2, \phi.\text{sub}.2), \dots, (\theta.\text{sub}.K, \phi.\text{sub}.K)\}$ directions, $\theta.\text{sub}.k$ and $\phi.\text{sub}.k$ are respectively an azimuth angle and an elevation angle of a k th incident signal source, $k=1, 2, \dots, K$, utilizing a three-dimensional tensor

$$(7) X_{\mathbb{P}_1} \in \mathbb{C}^{2M_x \times 2M_y \times T}$$

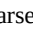
to express T sampling snapshot signals of a sparse uniform sub-surface array  custom character as follows:


(8) $X_{\mathbb{P}_1} = \text{Math. } a_x^{(\mathbb{P}_1)}(k, k) \circ a_y^{(\mathbb{P}_1)}(k, k) \circ s_k + N_{\mathbb{P}_1}$, wherein $s.\text{sub}.k=[s.\text{sub}.k,1, s.\text{sub}.k,2, \dots, s.\text{sub}.k,T].\text{sup}.T$ is a multi-snapshot sampling signal waveform corresponding to the k th incident signal source, $[\cdot].\text{sup}.T$ represents a transpose operation, \circ represents the outer product of a vector,  custom character is a noise tensor independent of each signal source,

(9) $a_x^{(\mathbb{P}_1)}(k, k)$ and $a_y^{(\mathbb{P}_1)}(k, k)$ are respectively steering vectors of  custom character in an x axial direction and a y axial direction, correspond to a signal source with an incoming wave direction of $(\theta.\text{sub}.k, \phi.\text{sub}.k)$, and are expressed as follows:

$$(10) a_x^{(\mathbb{P}_1)}(k, k) = [1, e^{-j x_{\mathbb{P}_1}^{(2)} k}, \text{Math. } e^{-j x_{\mathbb{P}_1}^{(2M_x)} k}]^T, a_y^{(\mathbb{P}_1)}(k, k) = [1, e^{-j y_{\mathbb{P}_1}^{(2)} v_k}, \text{Math. } e^{-j y_{\mathbb{P}_1}^{(2M_y)} v_k}]^T, \text{ and wherein}$$

$$(11) \{x_{\mathbb{P}_1}^{(1)}, x_{\mathbb{P}_1}^{(2)}, \text{Math. } x_{\mathbb{P}_1}^{(2M_x)}\} \{y_{\mathbb{P}_1}^{(1)}, y_{\mathbb{P}_1}^{(2)}, \text{Math. } y_{\mathbb{P}_1}^{(2M_y)}\} \quad (1)$$

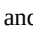
represent respectively actual positions of physical antenna elements of the sparse uniform sub-surface array  custom character in the x axial direction and y axial direction, and

(12) $x_{\mathbb{P}_1}^{(1)} = 0, y_{\mathbb{P}_1}^{(1)} = 0, k = \sin(\theta.\text{sub}.k) \cos(\phi.\text{sub}.k), v_k = \sin(\theta.\text{sub}.k) \sin(\phi.\text{sub}.k), j = \sqrt{-1}$; expressing the T sampled snapshot signals of the sparse uniform sub-surface array  custom character by another three-dimensional tensor

$$(13) X_{\mathbb{P}_2} \in \mathbb{C}^{N_x \times N_y \times T}$$

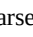
as follows:

$$(14) X_{\mathbb{P}_2} = \text{Math. } a_x^{(\mathbb{P}_2)}(k, k) \circ a_y^{(\mathbb{P}_2)}(k, k) \circ s_k + N_{\mathbb{P}_2}, \text{ wherein } \text{Math. } a_x^{(\mathbb{P}_2)}(k, k) \circ a_y^{(\mathbb{P}_2)}(k, k) \circ s_k + N_{\mathbb{P}_2} \text{ is a noise tensor independent of each signal source,}$$

(15) $a_x^{(\mathbb{P}_2)}(k, k)$ and $a_y^{(\mathbb{P}_2)}(k, k)$ are respectively steering vectors of  custom character in an x axial direction and a y axial direction, correspond to a signal source with an incoming wave direction of $(\theta.\text{sub}.k, \phi.\text{sub}.k)$, and are expressed as follows:

$$(16) a_x^{(\mathbb{P}_2)}(k, k) = [1, e^{-j x_{\mathbb{P}_2}^{(2)} k}, \text{Math. } e^{-j x_{\mathbb{P}_2}^{(N_x)} k}]^T, a_y^{(\mathbb{P}_2)}(k, k) = [1, e^{-j y_{\mathbb{P}_2}^{(2)} v_k}, \text{Math. } e^{-j y_{\mathbb{P}_2}^{(N_y)} v_k}]^T, \text{ and wherein}$$

$$(17) \{x_{\mathbb{P}_2}^{(1)}, x_{\mathbb{P}_2}^{(2)}, \text{Math. } x_{\mathbb{P}_2}^{(N_x)}\} \{y_{\mathbb{P}_2}^{(1)}, y_{\mathbb{P}_2}^{(2)}, \text{Math. } y_{\mathbb{P}_2}^{(N_y)}\}$$

represent respectively actual positions of physical antenna elements of the sparse uniform sub-surface array  custom character in the x axial direction and y axial direction, and

$$(18) x_{\mathbb{P}_2}^{(1)} = 0, y_{\mathbb{P}_2}^{(1)} = 0; \text{ obtaining a second-order cross-correlation tensor}$$

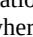
$$(19) R_{\mathbb{P}_1 \mathbb{P}_2} \in \mathbb{C}^{2M_x \times 2M_y \times N_x \times N_y}$$

by solving cross-correlation statistic of three-dimensional tensors  custom character and  custom character:


$$(20) R_{\mathbb{P}_1 \mathbb{P}_2} = E[\langle X_{\mathbb{P}_1}, X_{\mathbb{P}_2}^* \rangle_3] = \text{Math. } \sum_{k=1}^K a_x^{(\mathbb{P}_1)}(k, k) \circ a_y^{(\mathbb{P}_1)}(k, k) \circ a_x^{(\mathbb{P}_2)*}(k, k) \circ a_y^{(\mathbb{P}_2)*}(k, k) + N_{\mathbb{P}_1 \mathbb{P}_2}, \text{ wherein } \sum_{k=1}^K = E[s_k s_k^*]$$

represents power of a k th incident signal source,

$$(21) N_{\mathbb{P}_1 \mathbb{P}_2} = E[\langle N_{\mathbb{P}_1}, N_{\mathbb{P}_2}^* \rangle_3]$$

represents the cross-correlation noise tensor, $\langle \cdot, \cdot \rangle_{\text{sub}.r}$ represents a tensor contraction operation of the two tensors along a r th dimension, $E[\cdot]$ represents a mathematical expectation operation, and $(\cdot)^*$ represents a conjugation operation; the cross-correlation noise tensor  custom character only has an element with a value $\sigma.\text{sub}.n.\text{sup}.2$ in the $(1, 1, 1)$ th position, wherein $\sigma.\text{sub}.n.\text{sup}.2$ represents the noise power, and elements in other positions have the same value 0; (3) defining dimension sets $J.\text{sub}.1=\{1,3\}$, $J.\text{sub}.2=\{2,4\}$, and obtaining a virtual domain signal

$$(22) U_W \in \mathbb{C}^{2M_x N_x \times 2M_y N_y}$$

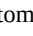

by performing a tensor transformation of dimension merging on the cross-correlation tensor  custom character:

$$(23) U_W = R_{\mathbb{P}_1 \mathbb{P}_2 \text{sub}.J_1 J_2} = \text{Math. } \sum_{k=1}^K b_x(k) \circ b_y(k), \text{ wherein by respectively forming a difference set array on the exponential term,}$$

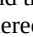
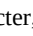
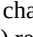
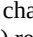
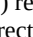


$$(24) b_x(k) = a_x^{(\mathbb{P}_2)*}(k, k) \cdot \text{Math. } a_x^{(\mathbb{P}_1)}(k, k) \text{ and } b_y(k) = a_y^{(\mathbb{P}_2)*}(k, k) \cdot \text{Math. } a_y^{(\mathbb{P}_1)}(k, k)$$

construct a two-dimensional augmented virtual surface array along the x axial direction and the y axial direction, \cdot represents the Kronecker product; therefore, $U.\text{sub}.W$ corresponds to a non-continuous virtual surface array W of size $J.\text{sub}.W.\text{sub}.x \times J.\text{sub}.W.\text{sub}.y$, $J.\text{sub}.W.\text{sub}.x=3M.\text{sub}.xN.\text{sub}.x-M.\text{sub}.x-N.\text{sub}.x+1$, $J.\text{sub}.W.\text{sub}.y=3M.\text{sub}.yN.\text{sub}.y-M.\text{sub}.y-N.\text{sub}.y+1$, and the non-continuous virtual surface array W contains holes in an entire row and an entire column, that is, missing elements; (4) constructing a virtual surface array W that mirrors the non-continuous virtual surface array W about the coordinate axis, and superimposing the W and W on a third dimension into a three-dimensional non-continuous virtual cubic array

$$(25) Q_{\text{ofsize}} J_{Q_x} \times J_{Q_y} \times J_{Q_z}, \text{ wherein } J_{Q_x} = J_{W_x}, J_{Q_y} = J_{W_y} \text{ and } J_{Q_z} = 2;$$

correspondingly, rearranging elements in the conjugate transposed signal $U.\text{sub}.W^*$ of the virtual domain signal $U.\text{sub}.W$ to correspond to positions of virtual array elements in W , so as to obtain a virtual domain signal $U.\text{sub}.W$ corresponding to the virtual surface array W ; superimposing $U.\text{sub}.W$ and $U.\text{sub}.W$ in the third dimension to obtain the virtual domain tensor  custom character corresponding to the non-continuous virtual cubic array  custom character, which is represented as:


$$(26) 0U_Q = \text{Math. } \sum_{k=1}^K \tilde{b}_x(k) \circ \tilde{b}_y(k) \circ c_k, \text{ wherein } \{\tilde{b}_x(k)\}.\text{sub}.x(k) \text{ and } \{\tilde{b}_y(k)\}.\text{sub}.y(k) \text{ are respectively steering vectors of the non-continuous virtual cubic array } \text{Math. } a_x^{(\mathbb{P}_2)*}(k, k) \circ a_x^{(\mathbb{P}_1)}(k, k) \text{ and } a_y^{(\mathbb{P}_2)*}(k, k) \circ a_y^{(\mathbb{P}_1)}(k, k) \text{ respectively correspond to elements in the hole positions in } \text{Math. } a_x^{(\mathbb{P}_2)*}(k, k) \circ a_x^{(\mathbb{P}_1)}(k, k) \text{ and } a_y^{(\mathbb{P}_2)*}(k, k) \circ a_y^{(\mathbb{P}_1)}(k, k) \text{ in the } x \text{ axial and } y \text{ axial directions which are set to be zero,}$$

(27) $c_k = [1, e^{-j (-(M_x M_y + M_x + M_y) k - (N_x N_y + N_x + N_y) v_k)}]^T$ represents a mirror transformation factor vector corresponding to W and W ; since the non-continuous virtual surface array W contains the holes in the entire row and the entire column, the non-continuous virtual cubic array  custom character obtained by superimposing W with a mirror image part thereof W contains contiguous holes, corresponds to virtual field tensor  custom character of the non-continuous virtual cubic array  custom character, and thus contains contiguous missing elements; (5) designing a translation window of size $P.\text{sub}.x \times P.\text{sub}.y \times 2$ to select a sub-tensor  custom character of the virtual domain tensor  custom character, which contains elements of which indices are $(1: P.\text{sub}.x-1)$, $(1: P.\text{sub}.y-1)$ and $(1:2)$ respectively in three dimensions of  custom character; then, translating the translation window by one element in turn along the x axial direction and the y axial direction, dividing  custom character into $L.\text{sub}.x \times L.\text{sub}.y$ sub-tensors, expressed as



(28) $U_{Q(s_x, s_y)}, S_x = 1, 2, \dots, L_x, S_y = 1, 2, \dots, L_y$,

wherein a value range of the translation window size is as follows:



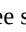
(29) $2 \leq P_x \leq J_{Q_x} - 1, 2 \leq P_y \leq J_{Q_y} - 1$, and $L_{\text{sub}.x}, L_{\text{sub}.y}, P_{\text{sub}.x}, P_{\text{sub}.y}$ satisfy the following relationship:

(30) $P_x + L_x - 1 = J_{Q_x}, P_y + L_y - 1 = J_{Q_y}$, superimposing the sub-tensors  custom character with the same index subscript $s_{\text{sub}.y}$ in the fourth dimension to obtain $L_{\text{sub}.y}$ four-dimensional tensors with $P_{\text{sub}.x} \times P_{\text{sub}.y} \times 2 \times L_{\text{sub}.x}$ dimensions; further, superimposing the $L_{\text{sub}.y}$ four-dimensional tensors in a fifth dimension to obtain a five-dimensional virtual domain tensor

(31) $T_Q \in \mathbb{C}^{P_x \times P_y \times 2 \times L_x \times L_y}$,


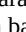


wherein the five-dimensional virtual domain tensor  custom character contains spatial angle information in the x axial direction and y axial direction, spatial mirror transformation information, and spatial translation information in the x axial direction and the y axial direction; defining the dimension sets $K_{\text{sub}.1}=\{1,2\}$, $K_{\text{sub}.2}=\{3\}$, $K_{\text{sub}.3}=\{4,5\}$, and merging through the dimensions of  custom character to obtain a three-dimensional reconstructed virtual domain tensor

(32) $K_Q \in \mathbb{C}^{P_x P_y \times L_x L_y \times 2}$;

(33) $K_Q \triangleq T_{Q_{(K_1, K_2, K_3)}}$ wherein the three dimensions of  custom character respectively represent the spatial angle information, the spatial translation information and the spatial mirror transformation information, thus, the contiguous missing elements in the original virtual domain tensor  custom character are randomly distributed to the three spatial dimensions contained in  custom character; (6) designing a virtual domain tensor filling optimization problem based on tensor kernel norm minimization:


(34) $\min_{K_Q} \text{Math. } \bar{K}_Q \cdot \text{Math. } s.t. P - (\bar{K}_Q) = P - (K_Q)$, wherein the optimization variable

(35) $K_Q \in \mathbb{C}^{P_x P_y \times L_x L_y \times 2}$


is the filled virtual domain tensor corresponding to the virtual uniform cubic array  custom character, $\|\cdot\|_{\text{sub}.*}$ represents the tensor kernel norm, Ω represents a position index set of the non-missing elements in  custom character, $P_{\text{sub}.Q}(\cdot)$ represents the mapping of the tensor on Ω ; since the kernel norm is a convex function, the virtual domain tensor filling problem based on the minimization of the tensor kernel norm is a solvable convex optimization problem, and wherein the convex optimization problem is solved to obtain  custom character; (7) expressing the filled virtual domain tensor  custom character as follows:


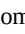

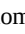

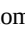
(36) 0


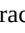

$\bar{K}_Q = \text{Math. } \bigotimes_{k=1}^K P_k \circ q_k \circ c_k$, wherein $p_k = d_y(k) \cdot \text{Math. } d_x(k), q_k = g_y(k) \cdot \text{Math. } g_x(k)$ are the space factors of $\bar{K}_Q, d_x(k) = [e^{j(-M_x N_x + M_x)}]_k, e^{j(-M_x N_x + M_x)}$

respectively represent the steering vectors of the virtual uniform cubic array  custom character along the x axial direction and y axial directions,

(37) $g_x(k) = [1, e^{j \dots}, \text{Math. } e^{j(L_x - 1) \dots}]^T, g_y(k) = [1, e^{j \dots}, \text{Math. } e^{j(L_y - 1) \dots}]^T$, are respectively spatial translation factor vectors


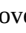
corresponding to the x axial direction and y axial direction in the process of intercepting the sub-tensor by the translation window; performing canonical polyadic decomposition on the filled virtual domain tensor  custom character to obtain the estimated values of three factor vectors $p_{\text{sub}.k}, q_{\text{sub}.k}$ and $c_{\text{sub}.k}$, which are expressed as $\{\text{circumflex over (p)}\}_{\text{sub}.k}, \{\text{circumflex over (q)}\}_{\text{sub}.k}$ and $\hat{c}_{\text{sub}.k}$; and extracting angle parameters contained in exponential terms of $\{\text{circumflex over (p)}\}_{\text{sub}.k}$ and $\{\text{circumflex over (q)}\}_{\text{sub}.k}$ to obtain a two-dimensional direction-of-arrival estimation result ($\{\text{circumflex over (theta)}\}_{\text{sub}.k}, \{\text{circumflex over (phi)}\}_{\text{sub}.k}$).

(38) Further, the coprime surface array structure described in step (1) is specifically described as follows: constructing a pair of sparse uniform sub-surface arrays  custom character and  custom character in a plane coordinate system xoy, wherein  custom character contains $2M_{\text{sub}.x} \times 2M_{\text{sub}.y}$ antenna elements, and the array element spacings in the x axial direction and the y axial direction are respectively $N_{\text{sub}.x}$ and $N_{\text{sub}.y}$, and position coordinate thereof on xoy is $\{(N_{\text{sub}.x}m_{\text{sub}.x}, N_{\text{sub}.y}m_{\text{sub}.y}) | m_{\text{sub}.x}=0, 1, \dots, 2M_{\text{sub}.x}-1, m_{\text{sub}.y}=0, 1, \dots, 2M_{\text{sub}.y}-1\}$;  custom character contains $N_{\text{sub}.x} \times N_{\text{sub}.y}$ antenna array elements, the array element spacings in the x axial direction and the y axial direction are respectively $M_{\text{sub}.x}$ and $M_{\text{sub}.y}$, and position coordinate thereof on xoy is $\{(M_{\text{sub}.x}n_{\text{sub}.x}, M_{\text{sub}.y}n_{\text{sub}.y}) | n_{\text{sub}.x}=0, 1, \dots, N_{\text{sub}.x}-1, n_{\text{sub}.y}=0, 1, \dots, N_{\text{sub}.y}-1\}$; $M_{\text{sub}.x}$ and $N_{\text{sub}.x}$, and $M_{\text{sub}.y}$ and $N_{\text{sub}.y}$ are respectively a pair of coprime integers; and combining the sub-arrays of  custom character and  custom character in the way that the array elements at (0, 0) position in the coordinate system overlap to obtain a coprime surface array that actually contains $4M_{\text{sub}.x}M_{\text{sub}.y} + N_{\text{sub}.x}N_{\text{sub}.y} - 1$ physical antenna array elements.

(39) Further, for the cross-correlation tensor derivation described in step (2), in practice, obtaining  custom character by calculating the cross-correlation statistic of the tensors  custom character and  custom character to approximate, that is, sampling cross-correlation tensor

(40) $\hat{R}_{P_1 P_2} \in \mathbb{C}^{2M_x \times 2M_y \times N_x \times N_y}$;

(41) $\hat{R}_{P_1 P_2} = \frac{1}{3} \cdot \text{Math. } X_{P_1}^*, X_{P_2}^* \cdot \text{Math. } \dots$

(42) Further, in step (7), performing the canonical polyadic decomposition on the filled virtual domain tensor  custom character to obtain the factor vectors $\{\text{circumflex over (p)}\}_{\text{sub}.k}, \{\text{circumflex over (q)}\}_{\text{sub}.k}$ and $\hat{c}_{\text{sub}.k}$, and, then extracting the parameters $\{\text{circumflex over (mu)}\}_{\text{sub}.k} = \sin(\{\text{circumflex over (phi)}\}_{\text{sub}.k}) \cos(\{\text{circumflex over (theta)}\}_{\text{sub}.k})$ and $\{\text{circumflex over (nu)}\}_{\text{sub}.k} = \sin(\phi_{\text{sub}.k}) \sin(\theta_{\text{sub}.k})$ from $\{\text{circumflex over (p)}\}_{\text{sub}.k}$  custom character $\{\text{circumflex over (q)}\}_{\text{sub}.k}$ as follows:

(43) $\hat{\mu}_k = (\angle(\frac{\hat{p}_{k_{(1,1)}}}{\hat{p}_{k_{(1,1)}}}) + \angle(\frac{\hat{q}_{k_{(1,1)}}}{\hat{q}_{k_{(1,1)}}})) / 2, \hat{\nu}_k = (\angle(\frac{\hat{p}_{k_{(2,1)}}}{\hat{p}_{k_{(2,1)}}}) + \angle(\frac{\hat{q}_{k_{(2,1)}}}{\hat{q}_{k_{(2,1)}}})) / 2$,

(44) wherein $\angle(\cdot)$ represents the operation of taking the argument of a complex number, and $a_{\text{sub}.a}$ represents the ath element of a vector a; here, according to the Kronecker structure of $\{\text{circumflex over (p)}\}_{\text{sub}.k}$ and $\{\text{circumflex over (q)}\}_{\text{sub}.k}$, $\eta_{\text{sub}.1} \in [1, P_{\text{sub}.x}P_{\text{sub}.y}-1]$ and $\eta_{\text{sub}.2} \in [1, L_{\text{sub}.x}L_{\text{sub}.y}-1]$ respectively satisfy $\text{mod}(\eta_{\text{sub}.1}, P_{\text{sub}.x}) \neq 0$ and $\text{mod}(\eta_{\text{sub}.2}, P_{\text{sub}.y}) \neq 0$, and $\delta_{\text{sub}.1} \in [1, P_{\text{sub}.x}P_{\text{sub}.y}-P_{\text{sub}.x}]$, $\delta_{\text{sub}.2} \in [1, L_{\text{sub}.x}L_{\text{sub}.y}-L_{\text{sub}.x}]$, $\text{mod}(\cdot)$ represents the operation of taking a remainder; according to the relationship between the parameter $(\mu_{\text{sub}.k}, \nu_{\text{sub}.k})$ and the two-dimensional direction-of-arrival $(\theta_{\text{sub}.k}, \phi_{\text{sub}.k})$, obtaining a closed-form solution of the two-dimensional direction-of-arrival estimation ($\{\text{circumflex over (theta)}\}_{\text{sub}.k}, \{\text{circumflex over (phi)}\}_{\text{sub}.k}$) as follows:

(45) $\hat{\theta}_k = \arctan(\frac{\hat{\nu}_k}{\hat{\mu}_k}), \hat{\phi}_k = \sqrt{\hat{\nu}_k^2 + \hat{\mu}_k^2}$.

(46) Compared with the prior art, the present invention has the following advantages: (1) The present invention derives the augmented non-continuous virtual surface array based on the cross-correlation tensor, and utilizes the mirror image expansion of the non-continuous virtual surface array to construct the three-dimensional non-continuous virtual cubic array and its corresponding virtual domain tensor, which fully preserves the structure information of all non-contiguous virtual domain statistics of the coprime array; (2) The present invention proposes a virtual domain tensor filling mechanism for the non-contiguous virtual arrays. The virtual field tensor is reconstructed to disperse its missing elements to meet the low-rank fallibility of the virtual domain tensor. The virtual domain tensor is effectively filled to achieve the high-precision and high-resolution two-dimensional direction-of-arrival estimation.

BRIEF DESCRIPTION OF THE DRAWINGS

(1) FIG. 1 is a general flow block diagram of the present invention.

(2) FIG. 2 is a schematic diagram of the structure of a coprime array constructed by the present invention.

(3) FIG. 3 is a schematic diagram of an augmented non-contiguous virtual surface array derived by the present invention.

(4) FIG. 4 is a schematic diagram of a non-contiguous virtual cubic array derived by the present invention.


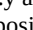
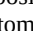
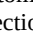
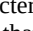
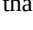
(5) FIG. 5 is a performance comparison diagram of the direction-of-arrival estimation accuracy of the method proposed in the present invention under different signal-to-noise ratio conditions.

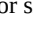
(6) FIG. 6 is a performance comparison diagram of the direction-of-arrival estimation accuracy of the method proposed in the present invention under different sampling snapshot numbers.

DESCRIPTION OF THE EMBODIMENTS

(7) The technical solution of the present invention will be described in further detail below with reference to the accompanying drawings.

(8) The present invention proposes a two-dimensional direction-of-arrival estimation method for a coprime surface array based on virtual domain tensor filling in order to solve the problems of loss of multi-dimensional signal structure information and inability to fully utilize virtual domain statistics in existing methods. Effective filling of contiguous missing elements of an original virtual domain tensor is used to realize a Nyquist-matched two-dimensional direction-of-arrival estimation of a coprime surface array. With reference to FIG. 1, the implementation steps of the present invention are as follows:

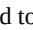
(9) Step 1: constructing a coprime surface array. Constructing a coprime surface array using $4M_{\text{sub.x}}M_{\text{sub.y}}+N_{\text{sub.x}}N_{\text{sub.y}}-1$ physical antenna array elements by a receiving end, as shown in FIG. 2: constructing a pair of sparse uniform sub-surface arrays  and  in a plane coordinate system xoy, wherein  contains $2M_{\text{sub.x}} \times 2M_{\text{sub.y}}$ antenna elements, and the array element spacings in the x axial direction and the y axial direction are respectively $N_{\text{sub.xd}}$ and $N_{\text{sub.yd}}$, and position coordinate thereof on xoy is $\{(N_{\text{sub.xdm}}\text{sub.x}, N_{\text{sub.ydm}}\text{sub.y}), m_{\text{sub.x}}=0, 1, \dots, 2M_{\text{sub.x}}-1, m_{\text{sub.y}}=0, 1, \dots, 2M_{\text{sub.y}}-1\}$;  contains $N_{\text{sub.x}} \times N_{\text{sub.y}}$ antenna array elements, the array element spacings in the x axial direction and the y axial direction are respectively $M_{\text{sub.xd}}$ and $M_{\text{sub.yd}}$, and position coordinate thereof on xoy is $\{(M_{\text{sub.xdn}}\text{sub.x}, M_{\text{sub.ydn}}\text{sub.y}), n_{\text{sub.x}}=0, 1, \dots, N_{\text{sub.x}}-1, n_{\text{sub.y}}=0, 1, \dots, N_{\text{sub.y}}-1\}$; $M_{\text{sub.x}}$ and $N_{\text{sub.x}}$, and $M_{\text{sub.y}}$ and $N_{\text{sub.y}}$ are respectively a pair of coprime integers; taking the unit interval d as half of the wavelength λ of an incident narrowband signal, that is, $d=\lambda/2$; and combining the sub-arrays of  and  in the way that the array elements at (0,0) position in the coordinate system overlap to obtain a coprime surface array that actually contains $4M_{\text{sub.x}}M_{\text{sub.y}}+N_{\text{sub.x}}N_{\text{sub.y}}-1$ physical antenna array elements.

(10) Step 2: modeling a tensor of a received signal of the coprime surface array. Assuming that there are K far-field narrowband uncorrelated signal sources from $\{(\theta_{\text{sub.1}}, \phi_{\text{sub.1}}), (\theta_{\text{sub.2}}, \phi_{\text{sub.2}}), \dots, (\theta_{\text{sub.K}}, \phi_{\text{sub.K}})\}$ directions, $\theta_{\text{sub.k}}$ and $\phi_{\text{sub.k}}$ are respectively an azimuth angle and an elevation angle of a kth incident signal source, $k=1, 2, \dots, K$, superimposing the T sampling snapshot signals of the sparse uniform sub-surface array  in the coprime surface array in the third dimension to obtain a three-dimensional tensor signal

$$(11) X_{\mathbb{P}_1} \in \mathbb{C}^{2M_x \times 2M_y \times T},$$

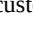
which is modeled as follows:

$$(12) X_{\mathbb{P}_1} = \sum_{k=1}^K \text{Math. } a_x^{(\mathbb{P}_1)}(k, k) \circ a_y^{(\mathbb{P}_1)}(k, k) \circ s_k + N_{\mathbb{P}_1}, \text{ wherein } s_{\text{sub.k}}=[s_{\text{sub.k},1}, s_{\text{sub.k},2}, \dots, s_{\text{sub.k},T}].\text{sup.T is a multi-snapshot sampling signal waveform corresponding to the kth incident signal source, } [\cdot].\text{sup.T represents a transpose operation, } \circ \text{ represents the outer product of a vector, } \text{Math. } a_x^{(\mathbb{P}_1)} \text{ is a noise tensor independent of each signal source,}$$

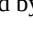
(13) $a_x^{(\mathbb{P}_1)}(k, k)$ and $a_y^{(\mathbb{P}_1)}(k, k)$ are respectively steering vectors of  in an x axial direction and a y axial direction, correspond to a signal source with an incoming wave direction of $(\theta_{\text{sub.k}}, \phi_{\text{sub.k}})$, and are expressed as follows:

$$(14) a_x^{(\mathbb{P}_1)}(k, k) = [1, e^{-j x_{\mathbb{P}_1}^{(2)} k}, \text{Math. } e^{-j x_{\mathbb{P}_1}^{(2M_x)} k}]^T, a_y^{(\mathbb{P}_1)}(k, k) = [1, e^{-j y_{\mathbb{P}_1}^{(2)} v_k}, \text{Math. } e^{-j y_{\mathbb{P}_1}^{(2M_y)} v_k}]^T, \text{ and wherein}$$

$$(15) 0 \{x_{\mathbb{P}_1}^{(1)}, x_{\mathbb{P}_1}^{(2)}, \text{Math. } x_{\mathbb{P}_1}^{(2M_x)}\} \{y_{\mathbb{P}_1}^{(1)}, y_{\mathbb{P}_1}^{(2)}, \text{Math. } y_{\mathbb{P}_1}^{(2M_y)}\}$$

represent respectively actual positions of physical antenna elements of the sparse uniform sub-surface array  in the x axial direction and y axial direction, and

$$(16) x_{\mathbb{P}_1}^{(1)} = 0, y_{\mathbb{P}_1}^{(1)} = 0, k = \sin(\theta_{\text{sub.k}}) \cos(\phi_{\text{sub.k}}), v_k = \sin(\theta_{\text{sub.k}}) \sin(\phi_{\text{sub.k}}), j = \sqrt{-1}.$$

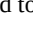
(17) Similarly, the received signals of the sparse uniform sub-surface array  can be expressed by three-dimensional tensor

$$(18) x_{\mathbb{P}_2} \in \mathbb{C}^{N_x \times N_y \times T}$$

as follows:

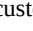
$$(19) X_{\mathbb{P}_2} = \sum_{k=1}^K \text{Math. } a_x^{(\mathbb{P}_2)}(k, k) \circ a_y^{(\mathbb{P}_2)}(k, k) \circ s_k + N_{\mathbb{P}_2}, \text{ wherein } \text{Math. } a_x^{(\mathbb{P}_2)} \text{ is a noise tensor independent of each signal source,}$$

$$(20) a_x^{(\mathbb{P}_2)}(k, k) \text{ and } a_y^{(\mathbb{P}_2)}(k, k)$$

are respectively steering vectors of  in an x axial direction and a y axial direction, correspond to a signal source with an incoming wave direction of $(\theta_{\text{sub.k}}, \phi_{\text{sub.k}})$, and are expressed as follows:

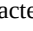

$$(21) a_x^{(\mathbb{P}_2)}(k, k) = [1, e^{-j x_{\mathbb{P}_2}^{(2)} k}, \text{Math. } e^{-j x_{\mathbb{P}_2}^{(N_x)} k}]^T, a_y^{(\mathbb{P}_2)}(k, k) = [1, e^{-j y_{\mathbb{P}_2}^{(2)} v_k}, \text{Math. } e^{-j y_{\mathbb{P}_2}^{(N_y)} v_k}]^T, \text{ and wherein}$$

$$(22) \{x_{\mathbb{P}_2}^{(1)}, x_{\mathbb{P}_2}^{(2)}, \text{Math. } x_{\mathbb{P}_2}^{(N_x)}\} \{y_{\mathbb{P}_2}^{(1)}, y_{\mathbb{P}_2}^{(2)}, \text{Math. } y_{\mathbb{P}_2}^{(N_y)}\}$$

represent respectively actual positions of physical antenna elements of the sparse uniform sub-surface array  in the x axial direction and y axial direction, and

$$(23) x_{\mathbb{P}_2}^{(1)} = 0, y_{\mathbb{P}_2}^{(1)} = 0. \text{ obtaining a second-order cross-correlation tensor}$$

$$(24) R_{\mathbb{P}_1 \mathbb{P}_2} \in \mathbb{C}^{2M_x \times 2M_y \times N_x \times N_y}$$

by solving cross-correlation statistic of three-dimensional tensor signals  and :

$$R_{\mathbb{P}_1 \mathbb{P}_2} = E[\text{Math. } X_{\mathbb{P}_1} X_{\mathbb{P}_2}^* \text{Math. }]$$

$$(25) = \sum_{k=1}^K \text{Math. } \frac{2}{k} a_x^{(\mathbb{P}_1)}(k, k) \circ a_y^{(\mathbb{P}_1)}(k, k) \circ a_x^{(\mathbb{P}_2)*}(k, k) \circ a_y^{(\mathbb{P}_2)*}(k, k) + \sigma_{\text{sub.k.sup.2}}, \text{ wherein } \sigma_{\text{sub.k.sup.2}} = E[s_{\text{sub.ks.sub.k}}^*] \text{ represents power of a kth incident signal source,}$$

(26) $0N_{\mathbb{P}_1 \mathbb{P}_2} = E[\text{Math. } N_{\mathbb{P}_1} N_{\mathbb{P}_2}^* \text{Math. }]$

represents the cross-correlation noise tensor, $\langle \cdot, \cdot \rangle_{\text{sub.r}}$ represents a tensor contraction operation of the two tensors along a rth dimension, $E[\cdot]$ represents a mathematical expectation operation, and $(\cdot)^*$ represents a conjugation operation. Here, the cross-correlation noise tensor  only has an element with a value $\sigma_{\text{sub.n.sup.2}}$ in the (1, 1, 1, 1)th position, wherein $\sigma_{\text{sub.n.sup.2}}$ represents the noise power, and

elements in other positions have the same value 0. In practice, obtaining $\mathcal{C}_{\text{custom character}}$ the cross-correlation statistic of the tensors $\mathcal{C}_{\text{custom character}}$ and $\mathcal{C}_{\text{custom character}}$ to approximate, that is, sampling cross-correlation tensor

$$(27) \hat{R}_{\mathbb{P}_1 \mathbb{P}_2} \in \mathbb{C}^{2M_x \times 2M_y \times N_x \times N_y};$$

(28) $\hat{R}_{\mathbb{P}_1 \mathbb{P}_2} = \frac{1}{J} \cdot \text{Math.} X_{\mathbb{P}_1} X_{\mathbb{P}_2}^* \cdot \text{Math.}$; Step 3: constructing an augmented non-continuous virtual surface array based on the cross-correlation tensor transformation of the coprime surface array. Since the cross-correlation tensor $\mathcal{C}_{\text{custom character}}$ contains the spatial information corresponding to the two sparse uniform sub-surface arrays $\mathcal{C}_{\text{custom character}}$ and $\mathcal{C}_{\text{custom character}}$, by merging the dimensions representing the spatial information in the same direction in $\mathcal{C}_{\text{custom character}}$, the steering vectors corresponding to the two sparse uniform sub-surface arrays can form a difference set array in the exponential term so as to construct a two-dimensional augmented virtual surface array. Specifically, the first and third dimensions of the cross-correlation tensor $\mathcal{C}_{\text{custom character}}$ (represented by the steering vectors

$$(29) a_x^{(P_1)}(k, k) \text{ and } a_x^{(P_2)}(k, k)$$

represent the spatial information of the x axial direction, and the second and fourth dimensions (represented by the steering vectors

$$(30) a_y^{(P_1)}(k, k) \text{ and } a_y^{(P_2)}(k, k))$$

represent the spatial information of the y axial direction; for this reason, defining the dimension sets J.sub.1={1, 3}, J.sub.2={2, 4}, and obtaining a virtual domain signal

$$(31) U_W \in \mathbb{C}^{2M_x N_x \times 2M_y N_y}$$

by performing the tensor transformation of dimension merging on the cross-correlation tensor $\mathcal{C}_{\text{custom character}}$:

$$(32) U_W \triangleq R_{\mathbb{P}_1 \mathbb{P}_2} = \sum_{k=1}^K \text{Math.} b_x(k) \circ b_y(k), \text{ wherein the}$$

$$(33) b_x(k) = a_x^{(P_2)}(k, k) \cdot \text{Math.} a_x^{(P_1)}(k, k) \text{ and } b_y(k) = a_y^{(P_2)}(k, k) \cdot \text{Math.} a_y^{(P_1)}(k, k)$$

are equivalent to the steering vectors of the non-continuous virtual surface array W on the x axis and the y axis, which corresponds to the signal source with the incoming wave direction ($\theta_{\text{sub.k}}, \phi_{\text{sub.k}}$), and \cdot represents the Kronecker product. The non-contiguous virtual surface array W has a size of J.sub.W.sub.x×J.sub.W.sub.y, and contains the holes (that is, missing elements) in an entire row and an entire column, as shown in FIG. 3, J.sub.W.sub.x=3M.sub.xN.sub.x-M.sub.x-N.sub.x+1, J.sub.W.sub.y=3M.sub.yN.sub.y-M.sub.y-N.sub.y+1. Here, in order to simplify the derivation process, the cross-correlation noise tensor $\mathcal{C}_{\text{custom character}}$ is omitted in the theoretical modeling step of U.sub.W. However, in practice, since the sampled cross-correlation tensor $\mathcal{C}_{\text{custom character}}$ is used to replace the theoretical cross-correlation tensor $\mathcal{C}_{\text{custom character}}$, $\mathcal{C}_{\text{custom character}}$ is still contained in the statistical processing of virtual domain signals; Step 4: deriving the virtual domain tensor based on the mirror expansion of the non-contiguous virtual surface array. Constructing a virtual surface array W mirroring the non-continuous virtual surface array W about the coordinate axis, and superimposing the W and W on the third dimension to form a three-dimensional non-continuous virtual cubic array $\mathcal{C}_{\text{custom character}}$ of size $\mathcal{C}_{\text{custom character}}$, as shown in FIG. 4. Here,

$$(34) J_{Q_x} = J_{W_x}, J_{Q_y} = J_{W_y} \text{ and } J_{Q_z} = 2.$$

Correspondingly, arranging the elements in the conjugate transposed signal U.sub.W* of the virtual domain signal U.sub.W to correspond to the positions of the virtual array elements in W, so that the virtual domain signal U.sub.W corresponding to the virtual surface array W can be obtained; and superimposing the U.sub.W and U.sub.W on the third dimension, so as to obtain the virtual domain tensor U $\mathcal{C}_{\text{custom character.sub}}$ corresponding to the non-contiguous virtual cubic array $\mathcal{C}_{\text{custom character}}$, which is expressed as:

$$(35) U_Q = \sum_{k=1}^K \tilde{b}_x(k) \circ \tilde{b}_y(k) \circ c_k, \text{ wherein } \{\tilde{b}\}_{\text{sub.x}}(k) \text{ and } \{\tilde{b}\}_{\text{sub.y}}(k) \text{ are respectively steering vectors of the non-continuous virtual cubic array } \mathcal{C}_{\text{custom character}} \text{ on the x axis and the y axis, and correspond to the signal source with an incoming wave direction } (\theta_{\text{sub.k}}, \phi_{\text{sub.k}}); \text{ due to existence of the missing elements (holes) in } \mathcal{C}_{\text{custom character}}, \{\tilde{b}\}_{\text{sub.x}}(k) \text{ and } \{\tilde{b}\}_{\text{sub.y}}(k) \text{ respectively correspond to elements in the hole positions in } \mathcal{C}_{\text{custom character}} \text{ in the x axial and y axial directions which are set to be zero,}$$

(36) $0c_k = [1, e^{j(-M_x M_y + M_x + M_y)k - (N_x N_y + N_x + N_y)v_k}]^T$ represents a mirror transformation factor vector corresponding to W and W; since the non-continuous virtual surface array W contains the holes in the entire row and the entire column, the non-continuous virtual cubic array $\mathcal{C}_{\text{custom character}}$ obtained by superimposing W with a mirror image part thereof W contains contiguous holes, corresponds to virtual field tensor $\mathcal{C}_{\text{custom character}}$ of the non-continuous virtual cubic array $\mathcal{C}_{\text{custom character}}$, and thus contains contiguous missing elements; Step 5: dispersing contiguous missing elements thereof by virtual domain tensor reconstruction. In order to construct a virtual uniform cubic array to realize the Nyquist matched signal processing, it is necessary to fill the contiguous missing elements in the virtual domain tensor $\mathcal{C}_{\text{custom character}}$, so as to correspond to a virtual uniform cubic array $\mathcal{C}_{\text{custom character}}$. However, the low-rank tensor filling technique is premised on the random distribution of missing elements in the tensor, and cannot effectively fill the virtual domain tensor $\mathcal{C}_{\text{custom character}}$ with contiguous missing elements. For this reason, dispersing contiguous missing elements thereof by reconstructing virtual domain tensor $\mathcal{C}_{\text{custom character}}$. Specifically, designing a translation window of size P.sub.x×P.sub.y×2 to select a sub-tensor $\mathcal{C}_{\text{custom character}}$ of the virtual domain tensor $\mathcal{C}_{\text{custom character}}$, which contains elements of which indices are (1: P.sub.x-1), (1: P.sub.y-1) and (1:2) respectively in three dimensions of $\mathcal{C}_{\text{custom character}}$; then, translating the translation window by one element in turn along the x axial direction and the y axial direction, and dividing $\mathcal{C}_{\text{custom character}}$ into L.sub.x×L.sub.y sub-tensors, expressed as

$$(37) U_{Q(s_x, s_y)}, s_x = 1, 2, \dots, L_x, s_y = 1, 2, \dots, L_y.$$

A value range of the translation window size is as follows:

$$(38) 2 \leq P_x \leq J_{Q_x} - 1, 2 \leq P_y \leq J_{Q_y} - 1, \text{ and } L_{\text{sub.x}}, L_{\text{sub.y}}, P_{\text{sub.x}}, P_{\text{sub.y}} \text{ satisfy the following relationship:}$$

$$(39) P_x + L_x - 1 = J_{Q_x}, P_y + L_y - 1 = J_{Q_y},$$

(40) Superimposing the sub-tensors $\mathcal{C}_{\text{custom character}}$ with the same index subscript s.sub.y in the fourth dimension to obtain L.sub.y four-dimensional tensors with P.sub.x×P.sub.y×2×L.sub.x dimensions; further, superimposing the L.sub.y four-dimensional tensors in a fifth dimension to obtain a five-dimensional virtual domain tensor

$$(41) T_Q \in \mathbb{C}^{P_x \times P_y \times 2 \times L_x \times L_y},$$

wherein the five-dimensional virtual domain tensor $\mathcal{C}_{\text{custom character}}$ contains spatial angle information in the x axial direction and y axial direction, spatial mirror transformation information, and spatial translation information in the x axial direction and the y axial direction; and, merging $\mathcal{C}_{\text{custom character}}$ along the first and second dimensions representing the spatial angle information, and at the same time merging it along the fourth and fifth dimensions representing the spatial translation information, and retaining the third dimension representing the spatial mirror transformation information. Specifically, defining the dimension sets K.sub.1={1,2}, K.sub.2={3}, K.sub.3={4,5} and merging through the dimensions of $\mathcal{C}_{\text{custom character}}$ to obtain a three-dimensional reconstructed virtual domain tensor

$$(42) K_Q \in \mathbb{C}^{P_x P_y \times L_x L_y \times 2};$$

(43) $K_Q \triangleq T_{Q(K_1, K_2, K_3)}$, wherein the three dimensions of $\mathcal{C}_{\text{custom character}}$ respectively represent the spatial angle information, the spatial translation information and the spatial mirror transformation information, thus, the contiguous missing elements in the virtual domain tensor $\mathcal{C}_{\text{custom character}}$ are randomly distributed to the three spatial dimensions contained in $\mathcal{C}_{\text{custom character}}$; Step 6: performing virtual domain

tensor filling based on tensor kernel norm minimization. In order to fill the reconstructed virtual domain tensor $\tilde{\mathbf{K}}_{\bar{\Omega}}$ custom character, designing a virtual domain tensor filling optimization problem based on tensor kernel norm minimization as follows:

(44) $\min_{\tilde{\mathbf{K}}_{\bar{\Omega}}} \|\tilde{\mathbf{K}}_{\bar{\Omega}}\|_{\text{sub}} \cdot \text{Math. } s.t. P^-(\tilde{\mathbf{K}}_{\bar{\Omega}}) = P^-(\mathbf{K}_{\bar{\Omega}})$, wherein the optimization variable

$$(45) \tilde{\mathbf{K}}_{\bar{\Omega}} \in \mathbb{C}^{P_x P_y \times L_x L_y \times 2}$$

is the filled virtual domain tensor, corresponding to the virtual uniform cubic array $\tilde{\mathbf{K}}_{\bar{\Omega}}$ custom character, $\|\cdot\|_{\text{sub}}$ represents the tensor kernel norm, Ω represents a position index set of the non-missing elements in $\tilde{\mathbf{K}}_{\bar{\Omega}}$ custom character, $P.\text{sub}.\Omega(\cdot)$ represents the mapping of the tensor on Ω . Since the kernel norm is a convex function, the virtual domain tensor filling problem based on the minimization of the tensor kernel norm is a solvable convex optimization problem. The convex optimization problem is solved to obtain $\tilde{\mathbf{K}}_{\bar{\Omega}}$ custom character; Step 7: decomposing the filled virtual domain tensor to obtain the direction-of-arrival estimation result. Expressing the filled virtual domain tensor $\tilde{\mathbf{K}}_{\bar{\Omega}}$ custom character as follows:

$$(46) \tilde{\mathbf{K}}_{\bar{\Omega}} = \text{Math. } \sum_{k=1}^K \mathbf{p}_k \circ \mathbf{q}_k \circ \mathbf{c}_k, \text{ wherein } \mathbf{p}_k = \mathbf{d}_y(k) \cdot \text{Math. } \mathbf{d}_x(k), \mathbf{q}_k = \mathbf{g}_y(k) \cdot \text{Math. } \mathbf{g}_x(k) \text{ are the space factors of } \tilde{\mathbf{K}}_{\bar{\Omega}}, \mathbf{d}_x(k) = [e^{j(-M_x N_x + M_x)k}, e^{j(-M_x N_x + M_x)k}, \dots, e^{j(-M_x N_x + M_x)k}]^T$$

respectively represent the steering vectors of the virtual uniform cubic array $\tilde{\mathbf{K}}_{\bar{\Omega}}$ custom character along the x axial direction and y axial directions,

(47) $\mathbf{0}_{g_x}(k) = [1, e^{j(-M_x N_x + M_x)k}, \dots, e^{j(-M_x N_x + M_x)k}]^T$, $\mathbf{0}_{g_y}(k) = [1, e^{j(-M_y N_y + M_y)k}, \dots, e^{j(-M_y N_y + M_y)k}]^T$, are respectively the spatial translation factor vectors corresponding to the x axial direction and y axial direction in the process of intercepting the sub-tensor by the translation window. Performing the canonical polyadic decomposition on the filled virtual domain tensor $\tilde{\mathbf{K}}_{\bar{\Omega}}$ custom character to obtain estimated values of the factor vectors $\mathbf{p}.\text{sub}.k$, $\mathbf{q}.\text{sub}.k$ and $\mathbf{c}.\text{sub}.k$, which are represented as $\{\text{circumflex over (p)}\}.\text{sub}.k$, $\{\text{circumflex over (q)}\}.\text{sub}.k$ and $\hat{\mathbf{c}}.\text{sub}.k$, and, then extracting the parameters $\{\text{circumflex over (mu)}\}.\text{sub}.k = \sin(\{\text{circumflex over (phi)}\}.\text{sub}.k) \cos(\{\text{circumflex over (theta)}\}.\text{sub}.k)$ and $\{\text{circumflex over (v)}\}.\text{sub}.k = \sin(\{\text{circumflex over (phi)}\}.\text{sub}.k) \sin(\{\text{circumflex over (theta)}\}.\text{sub}.k)$ from $\{\text{circumflex over (p)}\}.\text{sub}.k$ and $\{\text{circumflex over (q)}\}.\text{sub}.k$ as follows:

$$(48) \hat{\mu}_k = (\angle(\frac{\hat{p}_{k,1} + j\hat{p}_{k,2}}{\hat{p}_{k,1} - j\hat{p}_{k,2}}) + \angle(\frac{\hat{q}_{k,1} + j\hat{q}_{k,2}}{\hat{q}_{k,1} - j\hat{q}_{k,2}})) / 2, \hat{v}_k = (\angle(\frac{\hat{p}_{k,3} + j\hat{p}_{k,4}}{\hat{p}_{k,3} - j\hat{p}_{k,4}}) + \angle(\frac{\hat{q}_{k,3} + j\hat{q}_{k,4}}{\hat{q}_{k,3} - j\hat{q}_{k,4}})) / 2, \text{ wherein } \angle(\cdot) \text{ represents the operation of taking the argument of a}$$

complex number, and $\mathbf{a}.\text{sub}.a$ represents the ath element of a vector \mathbf{a} ; here, according to the Kronecker structure of $\{\text{circumflex over (p)}\}.\text{sub}.k$ and $\{\text{circumflex over (q)}\}.\text{sub}.k$, $\eta.\text{sub}.1 \in [1, P.\text{sub}.x P.\text{sub}.y - 1]$ and $\eta.\text{sub}.2 \in [1, L.\text{sub}.x L.\text{sub}.y - 1]$ respectively satisfy $\text{mod}(\eta.\text{sub}.1, P.\text{sub}.x) \neq 0$ and $\text{mod}(\eta.\text{sub}.2, P.\text{sub}.y) \neq 0$, and $\delta.\text{sub}.1 \in [1, P.\text{sub}.x P.\text{sub}.y - P.\text{sub}.x]$, $\delta.\text{sub}.2 \in [1, L.\text{sub}.x L.\text{sub}.y - L.\text{sub}.x]$, $\text{mod}(\cdot)$ represents the operation of taking a remainder. According to the relationship between the parameter $(\mu.\text{sub}.k, v.\text{sub}.k)$ and the two-dimensional direction-of-arrival $(\theta.\text{sub}.k, \phi.\text{sub}.k)$, obtaining a closed-form solution of the two-dimensional direction-of-arrival estimation $(\{\text{circumflex over (theta)}\}.\text{sub}.k, \{\text{circumflex over (phi)}\}.\text{sub}.k)$ as follows:

$$(49) \hat{\mu}_k = \arctan(\frac{\hat{v}_k}{\hat{\mu}_k}), \hat{v}_k = \sqrt{\hat{\mu}_k^2 + \hat{v}_k^2}.$$

(50) The effect of the present invention will be further described below in conjunction with a simulation example.

(51) Simulation example: the coprime array is used to receive an incident signal, and its parameters are selected as $M.\text{sub}.x=2$, $M.\text{sub}.y=3$, $N.\text{sub}.x=3$, $N.\text{sub}.y=4$, that is, the constructed coprime surface array contains $4M.\text{sub}.x M.\text{sub}.y + N.\text{sub}.x N.\text{sub}.y - 1 = 35$ physical array elements. The translation window size of the sub-tensor is $6 \times 15 \times 2$. Assuming that there are 2 narrowband incident signals, the azimuth and elevation angles of the incident direction are respectively $[30.6^\circ, 25.6^\circ]$ and $[40.5^\circ, 50.5^\circ]$. Comparing the two-dimensional direction-of-arrival estimation method of coprime surface array based on virtual domain tensor filling proposed by the present invention with the traditional Multiple Signal Classification (MUSIC) method and Tensor Multiple Signal Classification (Tensor MUSIC) method which only utilize the contiguous part of the virtual domain, under the condition of the number of sampling snapshots $T=300$, plotting performance comparison curves of Root Mean Square Error (RMSE) as a function of signal-to-noise ratio (SNR), as shown in FIG. 5; under the condition of SNR=0 dB, plotting performance comparison curves of RMSE as a function of the number of sampling snapshots T , as shown in FIG. 6.

(52) It can be seen from the comparison results of FIG. 5 and FIG. 6 that no matter in different expected signal-to-noise ratio (SNR) scenarios or in different numbers of the sampling snapshots T scenarios, the method proposed in the present invention has a performance advantage in the direction-of-arrival estimation accuracy. Compared with the traditional MUSIC method, the method proposed in the present invention makes full use of the structural information of the received signal of the coprime surface array by constructing the virtual domain tensor, so as to have better performance of direction-of-arrival estimation; and, compared with the Tensor MUSIC method, the performance advantage of the method proposed in the present invention comes from the use of all non-contiguous virtual domain statistics information through the virtual domain tensor filling, while the Tensor MUSIC method only extracts the continuous part of the non-contiguous virtual array for the virtual domain signal processing, resulting in loss of the virtual domain statistics information.

(53) In summary, the present invention realizes the random distribution of the contiguous missing elements through the virtual domain tensor reconstruction, and based on this, designs the virtual domain tensor filling method based on the tensor kernel norm minimization, and successfully utilizes all the non-contiguous virtual domain statistics information, which realizes the high-precision two-dimensional direction-of-arrival estimation of the coprime surface array.

(54) The above descriptions are only preferred embodiments of the present invention. Although the present invention has been disclosed above with preferred embodiments, they are not intended to limit the present invention. Any person skilled in the art, without departing from the scope of the technical solution of the present invention, can make many possible changes and modifications to the technical solution of the present invention by using the methods and technical contents disclosed above, or modify the technical solution of the present invention into equivalent examples. Therefore, any simple modification, equivalent change and modification made to the above embodiments according to the technical essence of the present invention without departing from the contents of the technical solution of the present invention still falls within the protection scope of the technical solution of the present invention.

Claims

1. A two-dimensional direction-of-arrival estimation method for a coprime surface array based on virtual domain tensor filling, wherein the method comprises the following steps: (1) configuring a receiving end with a coprime surface array by using $4M.\text{sub}.x M.\text{sub}.y + N.\text{sub}.x N.\text{sub}.y - 1$ physical antenna array elements, wherein $M.\text{sub}.x$, $N.\text{sub}.x$ and $M.\text{sub}.y$, $N.\text{sub}.y$ are a pair of coprime integers respectively; decomposing the coprime surface array into two sparse uniform sub-surface arrays $\tilde{\mathbf{K}}_{\bar{\Omega}}$ custom character and $\tilde{\mathbf{K}}_{\bar{\Omega}}$ custom character, wherein $\tilde{\mathbf{K}}_{\bar{\Omega}}$ custom character contains $2M.\text{sub}.x \times 2M.\text{sub}.y$ antenna array elements, array element spacings in an x axial direction and a y axial direction are respectively $N.\text{sub}.x d$ and $N.\text{sub}.y d$, $\tilde{\mathbf{K}}_{\bar{\Omega}}$ custom character includes $N.\text{sub}.x \times N.\text{sub}.y$ antenna array elements, array element spacings in the x axial direction and the y axial direction are respectively $M.\text{sub}.x d$ and $M.\text{sub}.y d$, and an unit interval d is taken as half of wavelength λ of an incident narrowband signal; (2) if there are K far-field narrowband uncorrelated signal sources from $\{(\theta.\text{sub}.1, \phi.\text{sub}.1), (\theta.\text{sub}.2, \phi.\text{sub}.2), \dots, (\theta.\text{sub}.K, \phi.\text{sub}.K)\}$ directions, $\theta.\text{sub}.k$ and $\phi.\text{sub}.k$ are respectively an azimuth angle and an elevation angle of a kth incident signal source, $k=1, 2, \dots, K$, utilizing a three-dimensional tensor $\mathbf{X}_{\mathbf{p}_1} \in \mathbb{C}^{2M_x \times 2M_y \times T}$ to express T sampling snapshot signals of a sparse uniform sub-surface array $\tilde{\mathbf{K}}_{\bar{\Omega}}$ custom character as follows:

$X_{\mathbb{P}_1} = \text{Math.} \sum_{k=1}^K a_x^{(\mathbb{P}_1)}(k, k) \circ a_y^{(\mathbb{P}_1)}(k, k) \circ s_k + N_{\mathbb{P}_1}$, wherein $s_{\text{sub.k}} = [s_{\text{sub.k},1}, s_{\text{sub.k},2}, \dots, s_{\text{sub.k},T}]$. sup.T is a multi-snapshot sampling signal waveform corresponding to the k th incident signal source, $[\cdot]_{\text{sup.T}}$ represents a transpose operation, \circ represents an outer product of a vector, custom character is a noise tensor independent of each signal source, $a_x^{(\mathbb{P}_1)}(k, k)$ and $a_y^{(\mathbb{P}_1)}(k, k)$ are respectively steering vectors of custom character in the x axial direction and the y axial direction, correspond to a signal source with an incoming wave direction of $(\theta_{\text{sub.k}}, \phi_{\text{sub.k}})$, and are expressed as follows: $a_x^{(\mathbb{P}_1)}(k, k) = [1, e^{j x_{\mathbb{P}_1}^{(2)} k}, \text{Math.}, e^{j x_{\mathbb{P}_1}^{(2M_x)} k}]^T$, $a_y^{(\mathbb{P}_1)}(k, k) = [1, e^{j y_{\mathbb{P}_1}^{(2)} v_k}, \text{Math.}, e^{j y_{\mathbb{P}_1}^{(2M_y)} v_k}]^T$, and wherein $\{x_{\mathbb{P}_1}^{(1)}, x_{\mathbb{P}_1}^{(2)}, \text{Math.}, x_{\mathbb{P}_1}^{(2M_x)}\} \{y_{\mathbb{P}_1}^{(1)}, y_{\mathbb{P}_1}^{(2)}, \text{Math.}, y_{\mathbb{P}_1}^{(2M_y)}\}$ represent respectively actual positions of physical antenna elements of the sparse uniform sub-surface array custom character in the x axial direction and the y axial direction, and $x_{\mathbb{P}_1}^{(1)} = 0, y_{\mathbb{P}_1}^{(1)} = 0, k = \sin(\theta_{\text{sub.k}}) \cos(\phi_{\text{sub.k}}), v_k = \sin(\theta_{\text{sub.k}}) \sin(\phi_{\text{sub.k}}), j = \sqrt{-1}$; expressing the T sampled snapshot signals of the sparse uniform sub-surface array custom character by another three-dimensional tensor $X_{\mathbb{P}_2} \in \mathbb{C}^{N_x \times N_y \times T}$ as follows:

$X_{\mathbb{P}_2} = \text{Math.} \sum_{k=1}^K a_x^{(\mathbb{P}_2)}(k, k) \circ a_y^{(\mathbb{P}_2)}(k, k) \circ s_k + N_{\mathbb{P}_2}$, wherein custom character is a noise tensor independent of each signal source, $a_x^{(\mathbb{P}_2)}(k, k)$ and $a_y^{(\mathbb{P}_2)}(k, k)$ are respectively steering vectors of custom character in the x axial direction and the y axial direction, correspond to a signal source with an incoming wave direction of $(\theta_{\text{sub.k}}, \phi_{\text{sub.k}})$, and are expressed as follows:

$a_x^{(\mathbb{P}_2)}(k, k) = [1, e^{j x_{\mathbb{P}_2}^{(2)} k}, \text{Math.}, e^{j x_{\mathbb{P}_2}^{(N_x)} k}]^T$, $a_y^{(\mathbb{P}_2)}(k, k) = [1, e^{j y_{\mathbb{P}_2}^{(2)} v_k}, \text{Math.}, e^{j y_{\mathbb{P}_2}^{(N_y)} v_k}]^T$, and wherein $\{x_{\mathbb{P}_2}^{(1)}, x_{\mathbb{P}_2}^{(2)}, \text{Math.}, x_{\mathbb{P}_2}^{(N_x)}\} \{y_{\mathbb{P}_2}^{(1)}, y_{\mathbb{P}_2}^{(2)}, \text{Math.}, y_{\mathbb{P}_2}^{(N_y)}\}$ represent respectively actual positions of physical antenna elements of the sparse uniform sub-surface array custom character in the x axial direction and the y axial direction, and $x_{\mathbb{P}_2}^{(1)} = 0, y_{\mathbb{P}_2}^{(1)} = 0$; obtaining a second-order cross-correlation tensor $R_{\mathbb{P}_1 \mathbb{P}_2} \in \mathbb{C}^{2M_x \times 2M_y \times N_x \times N_y}$ by solving cross-correlation statistic of the three-dimensional tensors custom character and

$$R_{\mathbb{P}_1 \mathbb{P}_2} = E[\text{Math.} X_{\mathbb{P}_1} X_{\mathbb{P}_2}^* \text{Math.}]$$

custom character : $= \text{Math.} \sum_{k=1}^K \frac{2}{k} a_x^{(\mathbb{P}_1)}(k, k) \circ a_y^{(\mathbb{P}_1)}(k, k) \circ a_x^{(\mathbb{P}_2)*}(k, k) \circ a_y^{(\mathbb{P}_2)*}(k, k) +$, wherein $N_{\mathbb{P}_1 \mathbb{P}_2}$

$\sigma_{\text{sub.k}} \text{sup.2} = E[s_{\text{sub.k}} s_{\text{sub.k}}^*]$ represents power of a k th incident signal source, $N_{\mathbb{P}_1 \mathbb{P}_2} = E[\text{Math.} N_{\mathbb{P}_1} N_{\mathbb{P}_2}^* \text{Math.}]$ represents a cross-correlation noise tensor, $\langle \cdot, \cdot \rangle_{\text{sub.r}}$ represents a tensor contraction operation of two tensors along a r th dimension, $E[\cdot]$ represents a mathematical expectation operation, and $(\cdot)^*$ represents a conjugation operation; the cross-correlation noise tensor custom character only has an element with a value $\sigma_{\text{sub.n}} \text{sup.2}$ in the (1, 1, 1, 1)th position, wherein $\sigma_{\text{sub.n}} \text{sup.2}$ represents a noise power, and elements in other positions have the same value 0; (3) defining dimension sets $J_{\text{sub.1}} = \{1, 3\}$, $J_{\text{sub.2}} = \{2, 4\}$, and obtaining a virtual domain signal $U_W \in \mathbb{C}^{2M_x N_x \times 2M_y N_y}$ by performing a tensor transformation of dimension merging on the cross-correlation tensor custom character : $U_W \triangleq R_{\mathbb{P}_1 \mathbb{P}_2(J_{\text{sub.1}}, J_{\text{sub.2}})} = \text{Math.} \sum_{k=1}^K \frac{2}{k} b_x(k) \circ b_y(k)$, wherein by respectively forming a difference set array on an exponential term,

$b_x(k) = a_x^{(\mathbb{P}_2)*}(k, k) \text{Math.} a_x^{(\mathbb{P}_1)}(k, k)$ and $b_y(k) = a_y^{(\mathbb{P}_2)*}(k, k) \text{Math.} a_y^{(\mathbb{P}_1)}(k, k)$ configure a two-dimensional augmented virtual surface array along the x axial direction and the y axial direction, Math. represents a Kronecker product; therefore, $U_{\text{sub.W}}$ corresponds to a non-continuous virtual surface array W of size $J_{\text{sub.W}} \text{sub.x} \times J_{\text{sub.W}} \text{sub.y}$, $J_{\text{sub.W}} \text{sub.x} = 3M_{\text{sub.x}} N_{\text{sub.x}} - M_{\text{sub.x}} - N_{\text{sub.x}} + 1$, $J_{\text{sub.W}} \text{sub.y} = 3M_{\text{sub.y}} N_{\text{sub.y}} - M_{\text{sub.y}} - N_{\text{sub.y}} + 1$, and the non-continuous virtual surface array W contains holes in an entire row and an entire column; (4) configuring a virtual surface array W that mirrors the non-continuous virtual surface array W about a coordinate axis, and superimposing the W and W on a third dimension into a three-dimensional non-continuous virtual cubic array

\mathbb{Q} of size $J_{\mathbb{Q}_x} \times J_{\mathbb{Q}_y} \times J_{\mathbb{Q}_z}$, wherein $J_{\mathbb{Q}_x} = J_{W_x}, J_{\mathbb{Q}_y} = J_{W_y}$ and $J_{\mathbb{Q}_z} = 2$; correspondingly, rearranging elements in a conjugate transposed signal $U_{\text{sub.W}}^*$ of the virtual domain signal $U_{\text{sub.W}}$ to correspond to positions of virtual array elements in W , so as to obtain a virtual domain signal $U_{\text{sub.W}}$ corresponding to the virtual surface array W ; superimposing $U_{\text{sub.W}}$ and $U_{\text{sub.W}}$ in the third dimension to obtain a virtual domain tensor custom character corresponding to the non-continuous virtual cubic array custom character , which is represented as:

$U_{\mathbb{Q}} = \text{Math.} \sum_{k=1}^K \frac{2}{k} \tilde{b}_x \circ \tilde{b}_y(k) \circ c_k$, wherein $\{\tilde{b}_x\}_{\text{sub.x}(k)}$ and $\{\tilde{b}_y\}_{\text{sub.y}(k)}$ are respectively steering vectors of the non-continuous virtual cubic array custom character on the x axial direction and the y axial direction, and correspond to the signal source with the incoming wave direction $(\theta_{\text{sub.k}}, \phi_{\text{sub.k}})$; due to existence of the holes in custom character , $\{\tilde{b}_x\}_{\text{sub.x}(k)}$ and $\{\tilde{b}_y\}_{\text{sub.y}(k)}$ respectively correspond to elements in hole positions in custom character in the x axial direction and the y axial direction which are set to be zero, $c_k = [1, e^{j (-M_x M_y + M_x + M_y) k - (N_x N_y + N_x + N_y) v_k}]^T$ represents a mirror transformation factor vector corresponding to W and W ; since the non-continuous virtual surface array W contains the holes in the entire row and the entire column, the non-continuous virtual cubic array custom character obtained by superimposing W with a mirror image part thereof W contains contiguous holes, corresponds to virtual field tensor custom character of the non-continuous virtual cubic array custom character , and thus contains contiguous missing elements; (5) designing a translation window of size $P_{\text{sub.x}} \times P_{\text{sub.y}} \times 2$ to select a sub-tensor custom character of the virtual domain tensor custom character , wherein custom character contains elements of which indices are (1: $P_{\text{sub.x}} - 1$), (1: $P_{\text{sub.y}} - 1$) and (1:2) respectively in three dimensions of custom character ; then, translating the translation window by one element in turn along the x axial direction and the y axial direction, dividing custom character into $L_{\text{sub.x}} \times L_{\text{sub.y}}$ sub-tensors, expressed as custom character , $s_{\text{sub.x}} = 1, 2, \dots, L_{\text{sub.x}}$, $s_{\text{sub.y}} = 1, 2, \dots, L_{\text{sub.y}}$, wherein a value range of a size of the translation window is as follows: $2 \leq P_x \leq J_{\mathbb{Q}_x} - 1, 2 \leq P_y \leq J_{\mathbb{Q}_y} - 1$, and $L_{\text{sub.x}}, L_{\text{sub.y}}, P_{\text{sub.x}}, P_{\text{sub.y}}$ satisfy the following relationship: $P_x + L_x - 1 = J_{\mathbb{Q}_x}, P_y + L_y - 1 = J_{\mathbb{Q}_y}$, superimposing the sub-tensors custom character with the same index subscript $s_{\text{sub.y}}$ in a fourth dimension to obtain $L_{\text{sub.y}}$ four-dimensional tensors with $P_{\text{sub.x}} \times P_{\text{sub.y}} \times 2 \times L_{\text{sub.x}}$ dimensions; further, superimposing the $L_{\text{sub.y}}$ four-dimensional tensors in a fifth dimension to obtain a five-dimensional virtual domain tensor $T_{\mathbb{Q}} \in \mathbb{C}^{P_x \times P_y \times 2 \times L_x \times L_y}$, wherein the five-dimensional virtual domain tensor custom character contains spatial angle information in the x axial direction and the y axial direction, spatial mirror transformation information, and spatial translation information in the x axial direction and the y axial direction; defining dimension sets $K_{\text{sub.1}} = \{1, 2\}$, $K_{\text{sub.2}} = \{3\}$, $K_{\text{sub.3}} = \{4, 5\}$, and merging through the dimensions of custom character to obtain a three-dimensional reconfigured virtual domain tensor $K_{\mathbb{Q}} \in \mathbb{C}^{P_x P_y \times L_x L_y \times 2}$; $K_{\mathbb{Q}} = T_{\mathbb{Q}_{(K_1, K_2, K_3)}}$ wherein the three dimensions of custom character respectively represent the spatial angle information, the spatial translation information and the spatial mirror transformation information, thus, the contiguous missing elements in the original virtual domain tensor custom character are randomly distributed to the three spatial dimensions contained in custom character ; (6) designing a virtual domain tensor filling optimization problem based on tensor kernel norm minimization: $\min_{K_{\mathbb{Q}}} \text{Math.} \bar{K}_{\mathbb{Q}} \text{Math.} s.t. P - (\bar{K}_{\mathbb{Q}}) = P - (K_{\mathbb{Q}})$, wherein optimization variable $K_{\mathbb{Q}} \in \mathbb{C}^{P_x P_y \times L_x L_y \times 2}$ is a filled virtual domain tensor corresponding to the virtual uniform cubic array custom character , $\|\cdot\|_{\text{sub.*}}$ represents a tensor kernel norm, Ω represents a position index set of non-missing elements in custom character , $P_{\text{sub.}\Omega}(\cdot)$ represents a mapping of a tensor on Ω , wherein the virtual domain tensor filling optimization

problem is solved to obtain $\tilde{\mathbf{K}}_Q$ custom character; (7) expressing the filled virtual domain tensor $\tilde{\mathbf{K}}_Q$ custom character as follows:

$\tilde{\mathbf{K}}_Q = \prod_{k=1}^K \mathbf{p}_k \circ \mathbf{q}_k \circ \mathbf{c}_k$, wherein $\mathbf{p}_{\text{sub}.k} = \mathbf{d}_{\text{sub}.y}(k) \cdot \mathbf{d}_{\text{sub}.x}(k)$, $\mathbf{q}_{\text{sub}.k} = \mathbf{g}_{\text{sub}.y}(k) \cdot \mathbf{g}_{\text{sub}.x}(k)$ are the space factors of $\tilde{\mathbf{K}}_Q$ custom character,

$\mathbf{d}_x(k) = [e^{j(-M_x N_x + M_x)k}, e^{j(-M_x N_x + M_x + 1)k}, \dots, e^{j(2M_x N_x - N_x)k}]^T$, $\mathbf{d}_y(k) = [e^{j(-M_y N_y + M_y)v_k}, e^{j(-M_y N_y + M_y + 1)v_k}, \dots, e^{j(2M_y N_y - N_y)v_k}]^T$,

respectively represent steering vectors of the virtual uniform cubic array $\tilde{\mathbf{K}}_Q$ custom character along the x axial direction and the y axial directions,

$\mathbf{g}_x(k) = [1, e^{j\pi p_k}, \dots, e^{j(L_x - 1)k}]^T$, $\mathbf{g}_y(k) = [1, e^{j\pi v_k}, \dots, e^{j(L_y - 1)v_k}]^T$, are respectively spatial translation factor vectors

corresponding to the x axial direction and the y axial direction in a process of intercepting the sub-tensor by the translation window; performing canonical polyadic decomposition on the filled virtual domain tensor $\tilde{\mathbf{K}}_Q$ custom character to obtain an estimated values of three factor vectors $\mathbf{p}_{\text{sub}.k}$, $\mathbf{q}_{\text{sub}.k}$ and $\mathbf{c}_{\text{sub}.k}$, which are expressed as $\{\text{circumflex over (p)}\}_{\text{sub}.k}$, $\{\text{circumflex over (q)}\}_{\text{sub}.k}$ and $\hat{\mathbf{c}}_{\text{sub}.k}$; and extracting angle parameters contained in exponential terms of $\{\text{circumflex over (p)}\}_{\text{sub}.k}$ and $\{\text{circumflex over (q)}\}_{\text{sub}.k}$ to obtain a two-dimensional direction-of-arrival estimation result ($\{\text{circumflex over (theta)}\}_{\text{sub}.k}$, $\varphi_{\text{sub}.k}$), wherein the receiving end with the coprime surface array steers, based on the two-dimensional direction-of-arrival estimation result ($\{\text{circumflex over (theta)}\}_{\text{sub}.k}$, $\{\text{circumflex over (phi)}\}_{\text{sub}.k}$), vectors corresponding to the signal source with the incoming wave direction ($\theta_{\text{sub}.k}$, $\varphi_{\text{sub}.k}$).

2. The two-dimensional direction-of-arrival estimation method for a coprime surface array based on virtual domain tensor filling according to claim 1, wherein the coprime surface array structure described in the step (1) is specifically described as follows: configuring a pair of sparse uniform sub-surface arrays $\tilde{\mathbf{K}}_Q$ custom character and $\tilde{\mathbf{K}}_Q$ custom character in a plane coordinate system xoy, wherein $\tilde{\mathbf{K}}_Q$ custom character contains

$2M_{\text{sub}.x} \times 2M_{\text{sub}.y}$ antenna elements, and the array element spacings in the x axial direction and the y axial direction are respectively $N_{\text{sub}.x}$ and $N_{\text{sub}.y}$, and position coordinate thereof on xoy is $\{(N_{\text{sub}.x}m_{\text{sub}.x}, N_{\text{sub}.y}m_{\text{sub}.y}) | m_{\text{sub}.x} = 0, 1, \dots, 2M_{\text{sub}.x} - 1, m_{\text{sub}.y} = 0, 1, \dots, 2M_{\text{sub}.y} - 1\}$; $\tilde{\mathbf{K}}_Q$ custom character contains $N_{\text{sub}.x} \times N_{\text{sub}.y}$ antenna array elements, the array element spacings in the x axial direction and the y axial direction are respectively $M_{\text{sub}.x}$ and $M_{\text{sub}.y}$, and position coordinate thereof on xoy is $\{(M_{\text{sub}.x}n_{\text{sub}.x}, M_{\text{sub}.y}n_{\text{sub}.y}) | n_{\text{sub}.x} = 0, 1, \dots, N_{\text{sub}.x} - 1, n_{\text{sub}.y} = 0, 1, \dots, N_{\text{sub}.y} - 1\}$; $M_{\text{sub}.x}$ and $N_{\text{sub}.x}$, and $M_{\text{sub}.y}$ and $N_{\text{sub}.y}$ are respectively a pair of coprime integers; and

combining the sub-arrays of $\tilde{\mathbf{K}}_Q$ custom character and $\tilde{\mathbf{K}}_Q$ custom character in the way that the array elements at (0, 0) position in the coordinate system overlap to obtain a coprime surface array that actually contains $4M_{\text{sub}.x}M_{\text{sub}.y} + N_{\text{sub}.x}N_{\text{sub}.y} - 1$ physical antenna array elements.

3. The two-dimensional direction-of-arrival estimation method for a coprime surface array based on virtual domain tensor filling according to claim 1, wherein for the cross-correlation tensor derivation described in the step (2), obtaining $\tilde{\mathbf{K}}_Q$ custom character by calculating the cross-correlation statistic of the tensors $\tilde{\mathbf{K}}_Q$ custom character and $\tilde{\mathbf{K}}_Q$ custom character to approximate, that is, sampling cross-correlation tensor

$$\hat{\mathbf{R}}_{\mathbb{P}_1 \mathbb{P}_2} \in \mathbb{C}^{2M_x \times 2M_y \times N_x \times N_y}; \hat{\mathbf{R}}_{\mathbb{P}_1 \mathbb{P}_2} = \frac{1}{T} \langle \mathbf{X}_{\mathbb{P}_1}, \mathbf{X}_{\mathbb{P}_2}^* \rangle.$$

4. The two-dimensional direction-of-arrival estimation method for a coprime surface array based on virtual domain tensor filling according to claim 1, wherein in the step (7), performing the canonical polyadic decomposition on the filled virtual domain tensor $\tilde{\mathbf{K}}_Q$ custom character to obtain the factor vectors $\{\text{circumflex over (p)}\}_{\text{sub}.k}$, $\{\text{circumflex over (q)}\}_{\text{sub}.k}$ and $\hat{\mathbf{c}}_{\text{sub}.k}$, and, then extracting the parameters $\{\text{circumflex over (mu)}\}_{\text{sub}.k} = \sin(\{\text{circumflex over (phi)}\}_{\text{sub}.k})\cos(\{\text{circumflex over (theta)}\}_{\text{sub}.k})$ and $\{\text{circumflex over (nu)}\}_{\text{sub}.k} = \sin(\varphi_{\text{sub}.k})\sin(\theta_{\text{sub}.k})$ from $\mathbf{p}_{\text{sub}.k}$

$\tilde{\mathbf{K}}_Q$ custom character $\{\text{circumflex over (q)}\}_{\text{sub}.k}$ as follows: $\hat{\mu}_k = (\angle(\frac{\hat{p}_{k(1,1)}}{\hat{p}_{k(1,1)}}) + \angle(\frac{\hat{q}_{k(1,1)}}{\hat{q}_{k(1,1)}})) / 2$, $\hat{\nu}_k = (\angle(\frac{\hat{p}_{k(2,1)}}{\hat{p}_{k(2,1)}}) + \angle(\frac{\hat{q}_{k(2,1)}}{\hat{q}_{k(2,1)}})) / 2$, wherein $\angle(\cdot)$

represents an operation of taking an argument of a complex number, and $\mathbf{a}_{\text{sub}.a}$ represents the ath element of a vector a; here, according to a Kronecker structure of $\{\text{circumflex over (p)}\}_{\text{sub}.k}$ and $\{\text{circumflex over (q)}\}_{\text{sub}.k}$, $\eta_{\text{sub}.1} \in [1, P_{\text{sub}.x}P_{\text{sub}.y} - 1]$ and $\eta_{\text{sub}.2} \in [1, L_{\text{sub}.x}L_{\text{sub}.y} - 1]$ respectively satisfy $\text{mod}(\eta_{\text{sub}.1}, P_{\text{sub}.x}) \neq 0$ and $\text{mod}(\eta_{\text{sub}.2}, P_{\text{sub}.y}) \neq 0$, and $\delta_{\text{sub}.1} \in [1, P_{\text{sub}.x}P_{\text{sub}.y} - P_{\text{sub}.x}]$, $\delta_{\text{sub}.2} \in [1, L_{\text{sub}.x}L_{\text{sub}.y} - L_{\text{sub}.x}]$, $\text{mod}(\ominus)$ represents an operation of taking a remainder; according to a relationship between the parameter ($\mu_{\text{sub}.k}$, $\nu_{\text{sub}.k}$) and a two-dimensional direction-of-arrival ($\theta_{\text{sub}.k}$, $\varphi_{\text{sub}.k}$), obtaining a closed-form solution of the two-dimensional direction-of-arrival estimation ($\{\text{circumflex over (theta)}\}_{\text{sub}.k}$, $\{\text{circumflex over (phi)}\}_{\text{sub}.k}$) as follows: $\hat{\theta}_k = \arctan(\frac{\hat{\nu}_k}{\hat{\mu}_k})$, $\hat{\varphi}_k = \sqrt{\hat{\mu}_k^2 + \hat{\nu}_k^2}$.